OPTICS OF THE CEBAF CW SUPERCONDUCTING ACCELERATOR*

R. C. York and D. R. Douglas
CEBAF, 12070 Jefferson Avenue, Newport News, VA 23606

Machine Overview

The CEBAF accelerator is designed as a recirculating cw linac to generate electron beams of energy 0.5 to 4.0 GeV at an emittance $\epsilon = 2 \times 10^{-9}$ m-rad with a momentum spread $(\sigma_E/E) = 2.5 \times 10^{-5}$. The machine, described elsewhere[1] and shown in Figure 1, consists of a 45 MeV injector, two superconducting cw linac segments, and a recirculator system. Each linac segment provides an energy gain of 0.5 GeV and simultaneously accelerates four beams at different energies. Each beam may be recirculated up to four times through both segments for a final energy of 4.0 GeV. The recirculator system consists of two 180° arcs that individually transport each beam energy from one linac segment to the other for further acceleration. In each arc, a "spreader" separates the beams according to energy. A set of beam lines (one for each energy) transports the beams to the next linac segment, where they are made collinear using a "recombiner" and injected into the linac segment.

The CEBAF beam transport system thus consists of five subsystems: linac lattices, spreaders, extraction regions, recirculation arc beam lines, and recombiners. The system design is driven by two issues. First, we require maximum stability of the beam against collective effects such as beam break up[2]. Secondly, degradation of beam quality is to be minimized. Dilution of the phase space may arise from synchrotron radiation excitation during recirculation or through optical errors such as mismatches of the beam phase space, distortions generated by optical aberrations in the beam lines, and perturbations due to imperfections in the magnetic fields that bend and focus the beam.

The CEBAF transport system is designed to address these issues and to be conceptually simple and operationally reliable. To this end, the magnetic lattice is modular with each module comprising one type of subsystem and has been treated to second order where appropriate. In this report, we focus on the idealized machine; machine performance and perturbation effects are discussed elsewhere[3].

Linac Beam Transport System

The linac beam transport system consists of a series of FODO cells in which are embedded "cryomodules" each containing eight superconducting accelerating cavities. Each cavity provides 2.5 MeV energy gain. The use of eight cavities per cryomodule is driven by cost considerations and by the desire to minimize the "head-tail" effect generated by the rf coupler[4]; this choice sets the cryomodule length of 8.4 m, which in turn determines the cell half-length of 9.4 m. A 1.0 m intercryomodule warm region is used for beam focusing, steering, and monitoring devices.

Each linac segment provides a 0.5 GeV energy gain by using 25 cryomodules; the transport system lattice of each segment thus comprises a total of 12 1/2 FODO cells. The recirculation transport lines between the first and second linac segments are tuned to provide imaging of the beam phase space between linacs. The linac segments therefore behave as a single contiguous linac consisting of 25 FODO cells containing 50 cryomodules. The quadrupoles are tuned to give a 120° phase advance per cell on the first pass. This choice provides stability against multi-pass beam break up and controls the beam envelope during multiple recirculations despite the reduced focal effect of the quadrupoles upon the higher-energy, recirculated beams.

A particular multiple-pass solution for the horizontal beam envelope is illustrated in Figure 2. As noted, the transport lines of the first arc are tuned to an identity transformation. The second arc transport lines are tuned to provide beam envelopes at the reinjection point that yield optimum beam behavior during the higher-energy passes. In this solution, the 45 MeV beam is injected with $\beta_x = 40.4$ m, $\alpha_x = 0.0$; each reinjected beam is brought to a waist at the center of the first quadrupole of linac 1 with a betatron function of ≈ 100 m.

Spreaders and Recombiners

Spreaders and recombiners are optically similar transport modules that serve to match beams of different energy between linac segments and arc transport lines. A spreader is shown in Figure 3. Upon leaving a linac segment, the four beams enter a common dipole and are differentially bent vertically according to their individual energies. Beyond this point, separate optical elements are utilized for each individual beam.

Along the paths of each of the three lowest-energy beams, a quadrupole triplet provides both horizontal and vertical focussing. A reverse bend then restores the path of the each beam to a separate trajectory parallel to, but vertically displaced from, the axis of the linac segment. The quadrupole triplet is configured to achromatize the vertical bending and to provide horizontal stability. Because the two bends are of opposite polarity, the vertical phase advance over the separating region is a full betatron wavelength. This system separates the beams in minimal distance with few magnetic elements but requires the use of strong quadrupoles, which cause severe modulation of the beam envelope. For this reason, a quadrupole doublet (focussing in both planes and serving to stabilize the beam envelope) follows the second vertical bend. Subsequently, each beam is individually matched to a specific recirculation transport line using a set of six matching quadrupoles. The use of six quadrupoles insures that a full transverse phase space match including betatron phase control is possible.

The highest-energy beam is treated differently. Following the common dipole and separating drift, the beam is achromatically returned to a path coincident with the linac axis by means of a vertical dogleg. A quadrupole doublet then stabilizes the beam envelope in both planes. Subsequently, a six-quadrupole matching section provides a phase space match to the arc beam line.

Recombiners are mirror images of spreaders. Individual beams from the arc transport lines are phase-matched to a linac segment using six quadrupoles. A quadrupole doublet then focuses the beam envelopes to prepare them for achromatic vertical bending; this restores all beams to the axis of the linac segment.

The use of these systems allows separation of beams of different energies and provides for individual phase matching of each beam to both a specific arc transport line and to the next linac segment. This flexibility is exploited by tuning the lines in the first recirculation arc to provide imaging of the phase space between the linac segments; the linac segments

*Supported by D.O.E. contract #DE-AC05-84ER4015

CH2387-9/87/0000-1292 $1.00 © IEEE

then function as a single contiguous linac. The beam lines in the second arc are tuned to provide beam envelopes at the reinjection point that give optimum beam envelope stability during recirculation. The beam envelopes in the spreader, extraction region, and recombiner of one recirculation path are illustrated in Figure 4.

Extraction Regions

Each recirculation beam line in the machine region adjacent to the experimental areas contains an extraction region between the spreader and the recirculation arc beam transport line. The extraction system is based on the use of rf separators which allow selective extraction of beam current at the microbunch level. An rf separator with a frequency of 2.5 GHz (the 5/3 harmonic of the linac frequency of 1.5 GHz) is located at the beginning of a pair of 90° FODO cells. The transfer matrix of the FODO cells is a negative identity, which maintains the optical match required for the recirculation arcs. The FODO cells are used as an optical amplifier to magnify the kick of the separator, allowing the use of conventional room-temperature rf technology.

To produce extracted beam at the energy of a particular recirculation line, the rf separator in that line is activated and every third microbunch is horizontally deflected by 100 μrad, creating a horizontal displacement of 5 mm at a thin septum positioned at the end of the first FODO cell. The thin septum imparts an additional 1 mrad kick to the extracted bunch, which is amplified by the second FODO cell. A second, thick, septum bends the extracted bunch clear of the recirculation path. The unextracted microbunches are deflected in a direction opposite to the extracted current and view the extraction channel as a simple half-wavelength orbit bump.

Using this scheme, it is possible to provide three simultaneous beams at correlated energies to three experimental areas. The energy combinations possible are: three beams at the highest energy, or two beams at the highest energy and one at any of the three possible lower energies, or one beam at the highest energy and two beams at any of the three possible lower energies.

Recirculation Arc Beam Lines[5]

The recirculator arc beam lines are designed to avoid degrading beam quality through error sensitivity, synchrotron radiation excitation, or optical aberrations. The two recirculation arcs comprise a total of seven beam lines; for a final energy of 4.0 GeV, the four lines in the first arc transport beams at 0.5, 1.5, 2.5 and 3.5 GeV, while the three lines in the second arc carry beams at 1.0, 2.0 and 3.0 GeV.

The requirement of minimal beam degradation implies two lattice constraints. The first is that the beam line lattices be achromatic, isochronous, imaging, and provide a total beam path length that is a multiple of the rf wavelength. These features facilitate both transverse and longitudinal matching between linacs and insure that no phase space dilution arises.

The second constraint imposed to avoid beam degradation is that the arcs minimize phase space degradation due to synchrotron radiation. The radiation-induced energy spread σ_E and emittance blowup $\Delta\epsilon$ occurring when a beam bends through 180° are given by:[6]

$$\sigma_E^2 = 1.182 \times 10^{-33}\mathrm{GeV}^2\mathrm{m}^2\frac{\gamma^7}{\rho^2}$$

$$\Delta\epsilon = 1.32\pi \times 10^{-27}\mathrm{m}^2\mathrm{rad}\frac{\gamma^5}{\rho^2}\langle\mathcal{H}\rangle$$

Here

$$\langle\mathcal{H}\rangle = (\frac{1}{L})\int_{\mathrm{bends}} ds\{(\frac{1}{\beta})[\eta^2 + (\beta\eta' - \frac{1}{2}\beta'\eta)^2]\}$$

with L= orbit length in bends and ρ= orbit radius in bends.

At a given energy, the σ_E is a function of the ρ only; $\Delta\epsilon$ is a function of both ρ and the betatron parameters. Thus, the bend radius in the highest-energy beam lines is set by the requirement that the momentum spread remain at the 10^{-4} level; the betatron parameters are then optimized to control the emittance degradation. In particular, the lattice is designed so as to keep the dispersion function η small in the dipoles, thereby reducing $\langle\mathcal{H}\rangle$. We find that ρ=30 m in the highest-energy beam lines will provide the desired momentum spread up to energies of 6 GeV.

Bending radii for lower-energy beam lines may be smaller, but are constrained by a desire for operational simplicity; all beam lines have therefore been designed similarly. Low-energy beam lines are generated from high-energy lines by replacing bending magnets with drift spaces and using reduced bending radii. Beam line focusing magnets are reset to retain the desired optical properties and the drift lengths are adjusted to yield a total beam path length equal to a multiple of the rf wavelength.

The transverse emittance blow-up is reduced by careful control of the dispersion. This was achieved, together with achromaticity, isochronicity, and imaging, through the use of a four-period structure in each beam line. Each period consists of a modified four-cell FODO structure with "missing magnets". Instead of a uniform distribution of dipoles, drift spaces are introduced, which allows the dispersion to cross the design orbit and create an isochronous structure. The use of four periods per line reduces both dispersion and betatron functions (thereby reducing $\langle\mathcal{H}\rangle$). As all lines are similar corresponding beam line elements all lie in approximately the same vertical plane.

Imaging is obtained by tuning each period to 5/4 betatron wavelength. This produces a unit transfer matrix over the arc and yields well-behaved lattice functions; the beam line is therefore resistant to perturbation effects. All linear chromatic aberrations and second order geometric aberrations are eliminated through the use of sextupoles. The beam lines are second-order achromats[7]. All periods of all lines have been matched to the same betatron function values, allowing all lines to be treated equivalently for matching purposes. The properties of each type of beam line are given in Table 1. As the focussing structures of all lines are similar, so are the lattice functions. They are illustrated in Figure 5 for one period of one beam line.

Table 1: Beam Line Lattice Properties

Lattice Property	0.5-2.0 GeV Lines	2.5 GeV Line	3.0-3.5 GeV Lines
# Dipoles	16	32	40
Orbit Radius in Dipoles (m)	11.46	22.92	28.65
Dipole Magnetic Length (m)	2.25	2.25	2.25
# Quadrupoles	31	31	31
Min. Quad Focal Length (m)	4.56	4.30	4.36
Phase Advances $\psi_{x,y}$	$2\pi \times 5$	$2\pi \times 5$	$2\pi \times 5$
Matched β_x, β_y (m)	35, 3.5	35, 3.5	35, 3.5
$\langle\mathcal{H}\rangle$ (m)	0.114	0.167	0.269
x,y natural chromaticities	-7.6,-8.11	-8.66,-7.76	-9.28,-7.92
# Sexupoles	8	8	8
Peak Sextupole $(B''l/B\rho)$ (m^2)	1.51	1.14	1.24

Figure 1. Schematic of CEBAF recirculating linac.

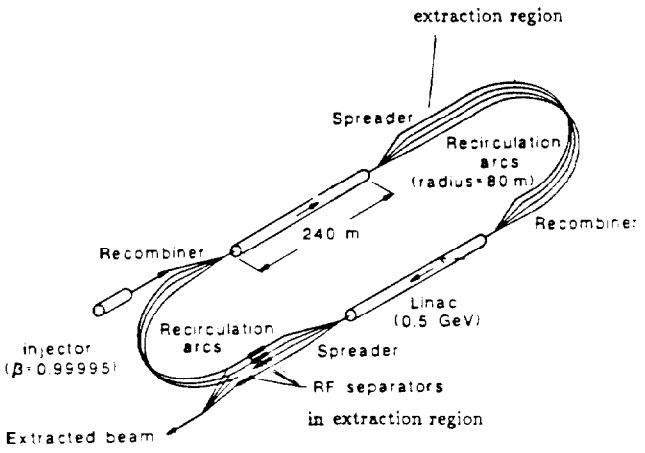

Figure 2. Horizontal beam envelope functions for all passes through linac segments. Each curve corresponds to the function $\beta_x = \sigma_x^2/\epsilon_{\text{injected}}$ on that pass, where $\epsilon_{\text{injected}}$ is the beam emittance at injection into linac 1 on the pass in question.

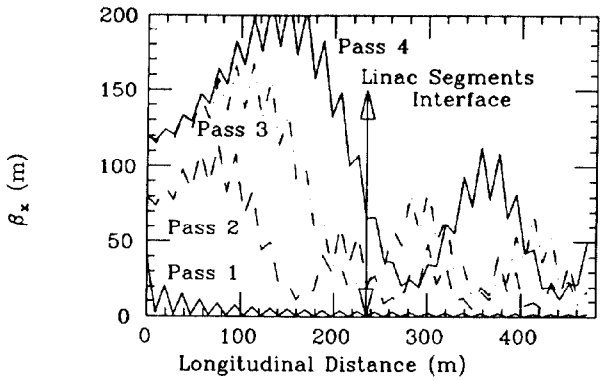

Figure 3. Side view of spreader.

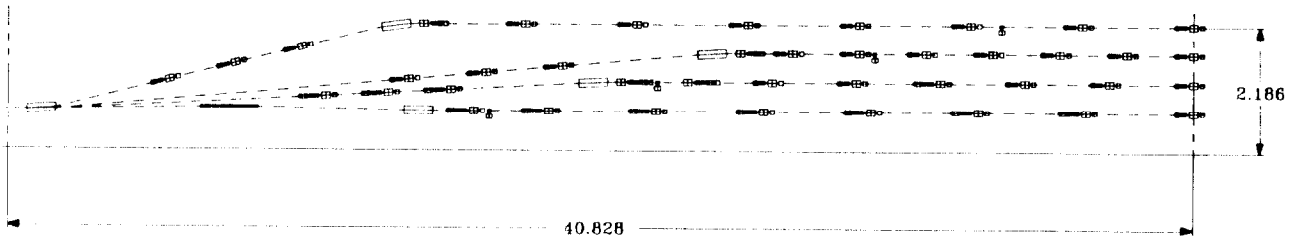

Figure 4. Beam envelopes in spreader, extraction region, and recombiner for 3.0 GeV recirculation transport line. Solid line corresponds to β_x, dashed line to β_y.

Figure 4a). Spreader and extraction region.

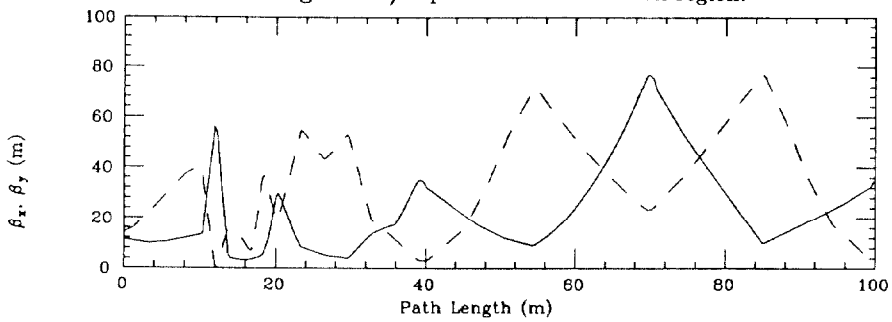

Figure 4b). Recombiner.

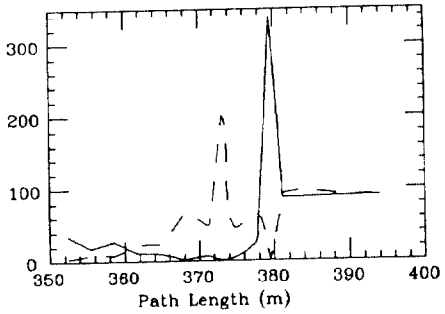

Figure 5. Layout and lattice functions for one period of highest-energy arc beam line.

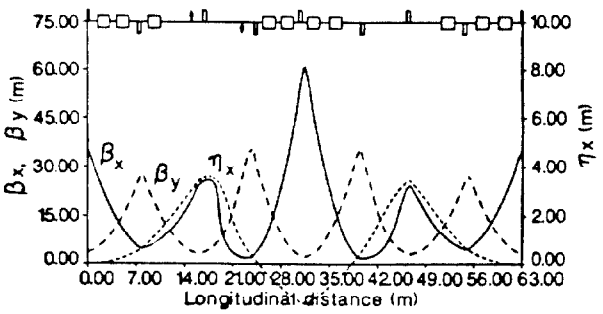

References

1. H. Grunder, these proceedings; Ch. Leemann, 1986 Linear Acc. Conf. Proc., SLAC-Report-303 (Sept. 1986).
2. J. J. Bisognano, R. L. Gluckstern, these proceedings; G. A. Krafft, J. J. Bisognano, these proceedings.
3. D. R. Douglas, R. C. York, these proceedings.
4. R. C. York, C. Reece, these proceedings.
5. D. R. Douglas, 1986 Linear Acc. Conf. Proc., SLAC-Report-303 (Sept. 1986) provides a detailed description.
6. M. Sands, SLAC-121 (Nov. 1970).
7. K. L. Brown, I.E.E.E. Trans. Nuc. Sci. NS-26, 3 (1979).